CrossMark
click for updates

Preparation and attachment of liquid-infused porous supra-particles to liquid interfaces

Hamza Al-Shehri, Tommy S. Horozov and Vesselin N. Paunov*

We prepared model porous composite supra-particles and investigated the effect of the initial infused fluid phase on their attachment at the liquid–fluid interface. We used a simple method for fabrication of millimetre-sized spherical porous supra-particles from much smaller monodisperse latex microparticles as building blocks by evaporation of a polystyrene sulphate latex suspension on a hot super-hydrophobic surface. We annealed the dried supra-particles at the polymer's glass transition temperature to fuse partially their latex particle building blocks. Spherical porous supra-particles were produced above 40 wt% initial concentration of the latex particles in the suspension, which had a rough surface, with a porous and amorphous structure. We controlled the supra-particle size by varying the initial volume of the latex suspension drop, the latex particle concentration and the drop evaporation temperature. This prepara-tion technique allowed limited control over the porosity of the supra-particles by varying the initial concentration of the latex particle suspension, the rate of evaporation and the annealing temperature. We characterised the surface morphology and the inner structure of supra-particles by SEM imaging. We report for the first time results of an MRI study of supra-particles attached to an air–water or an oil–water interface, which indicated that only the surface layer of the building block particles attaches to the liquid interface while the pore fluid was not displaced by the outer fluid. We observed that supra-particles infused with water had different wettability and attachment positions at the oil–water interface compared with the same particles infused with oil. Similarly, the infusion of the porous supra-particles with water led to a different attachment at the air–water interface compared to the attachment of the same supra-particle when dry. The fundamental importance of this result is that the porous particles (or colloid particle agglomerates) may give an oil-in-water or water-in-oil Pickering emulsion depending on whether they are initially impregnated with oil or water. The results of this study are relevant for particle-stabilised emulsions and foams in a range of pharmaceutical, food and cosmetic formulations as well as ore flotation.

Introduction

The wettability of powder particles by different liquids is very important for making pharmaceutical and cosmetic products, food, water treatments, building materials, paint, and for secondary oil recovery. The particle wettability is characterised by the particle contact angle (θ) which shows how the adsorbed particle "sits" at the liquid interface. The degree of wetting (wettability) of the particle is determined by a force balance between adhesive and cohesive forces but also depends on the particle porosity.

Porous particles have been used in numerous applications for decades. Porous particle applications include the production and development of pharmaceutical products, building materials, catalysts, sintered materials, ceramics, adsorbents, pigments, chromatography components, and filters. Each application

Department of Chemistry, University of Hull, Hull, HU67RX, UK.
*E-mail: v.n.paunov@hull.ac.uk; Fax: +44 (0)1482 466410; Tel: +44 (0)1482 465660*

seems to have an optimal specific pore size.[1] On the basis of size, pores are categorised into three classes: macropores (pore diameter: >50 nm), mesopores (pore diameter: 2–50 nm), and micropores (pore diameter: <2 nm).[2] Particles containing unsaturated bonds at their surfaces form a bigger loosely coherent particle known as an aggregate, owing to the presence of weak bonds. If the particles are rigidly combined, as could occur under the influence of temperature or pressure, these types of particles are termed agglomerates.[3–5]

A number of approaches have been developed to assemble inorganic or organic particles into a dense packing of colloidal particles. Several techniques have been used to arrange the particles into macroscopic spherical structures that can encap-sulate proteins, drugs, and other components; such arrangements are known as supra-particles, supra-balls, or colloidosomes.[6–16]

The aggregation of colloidal particles in three-dimensional structures can be achieved *via* the slow evaporation of droplet particle suspensions.[17] Researchers have proposed an emul-sion technique for the preparation of supra-particles from

monodisperse colloidal particle suspension templates[18,19] to manufacture microstructured hollow particles[20] and ball-like aggregates.[21] Another methodology for the production of porous supra-particles is the evaporation of a drop of particle suspension on super-hydrophobic surfaces. Particle crystal formation can be achieved by evaporating the droplet at room temperature. The size and shape of the particles depend on the droplet volume and the wettability of the surface.[7,22–24] This method has been used to create hemispherical particles,[24] spheroidal supra-balls,[17] photonic balls,[25,26] anisotropic particles,[27] dimpled particles, and doughnut-like structures.[7]

Velev *et al.*[7] evaporated droplets of particle suspension on the surface of fluorinated oil, which is immiscible with water. A Petri dish with Teflon tape on its wall was used to prevent meniscus formation between the oil and the Petri dish. This was important because meniscus formation could deform the droplet shape *via* capillary forces. The initial latex particle concentration of the microliter droplet was between 5 vol% and 30 vol%. Subsequently, the Petri dish with the drop was kept in a desiccating chamber for 12 hours. This procedure yielded spherical supra-particles of homogeneous size (100–500 μm) and appearance.[7] Highly ordered composite porous supra-particles with hexagonal arrangement had a volume packing fraction of <0.7404, representing the maximum packing fraction of monodisperse rigid spheres.

Another method involves the use of a colloidal suspension dried on a super-hydrophobic surface.[17,28] The super-hydrophobic surface was prepared *via* low-density polyethylene (LDPE), as it is hydrophobic against both the solvent (xylene) and non-solvent (methyl ethyl ketone). Methyl ethyl ketone was used to make the surface more rough, thus increasing the contact angle. The drop of the latex particle suspension decreased in volume during the 60 minute evaporation process and formed composite supra-particles built from closely packed mono-disperse particles.

Although there are countless examples about the importance of the attachment of porous particles or particle agglomerates to liquid surfaces, a very few studies have been conducted in a systematic manner to reveal the attachment mechanism. Cayre and Paunov[29] used the Gel Trapping Technique[30–32] to investigate the adsorption of porous gold microparticles as well as aggregates of hydrophobic silica particles at the air–water and the decane–water interface. The possible reasons for the lack of comprehensive studies of the mechanism of attachment of porous or complex particles is: (i) the lack of rigorous theoretical insights into the attachment mechanism of porous particles or particle aggregates; (ii) the lack of consistent geometry of particle aggregates which makes any study difficult to reproduce and test by other authors. To overcome these difficulties, model porous particles of well-characterised building blocks were fabricated, which allowed us to study consistently their wetting behaviour at liquid surfaces. We developed a new and simple method for the fabrication of model supra-particles built of smaller latex particles packed in a spherical aggregate. The microstructure of the obtained supra-particles was controlled by: (i) the initial volume fraction of the latex suspension, (ii) the drop evaporation rate at
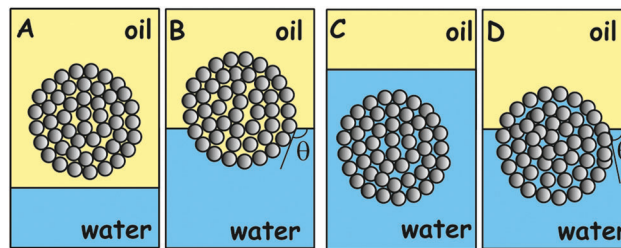
Scheme 1 Illustration of a supra-particle attached to the oil–water interface and infusion of the porous particles by one of the liquid phases upon their attachment. (A) A porous supra-particle filled with oil and (B) attached to the oil–water interface. (C) A supra-particle filled with water and (D) attached to the oil–water interface. The same applies for the air–water interface for pre-wet and for dry porous particles. Note that the same porous particles may have different effective contact angles depending on the infused fluid before their attachment to the liquid interface.

different temperatures in the range 60–105 °C, and (iii) the annealing temperature of the prepared composite supra-particles. The supra-particle size was controlled by the initial volume of the latex particle suspension for a fixed particle concentration. We studied the effect of the surface structure, porosity and the infusion of the porous particles by one of the fluid phases on their attachment to the liquid–fluid interfaces. Our aim was to find how the porous supra-particles attach to the liquid surface after being initially infused with one of the adjacent fluid phases. Scheme 1 summarises the main hypothesis of this study which was later confirmed by the MRI study of model porous particles prepared from monodisperse latex spherical particles, as described below.

The focus of this study was to reveal how porous particles which are pre-infused with a fluid attach to liquid surfaces. To achieve this goal we had to make stable model porous particles in a controllable way. Although the preparation of non-spherical rod- or disk-shaped particles could also be of interest, here we aim only to make spherical porous particles, to control the particle size and to study how they attach to liquid surfaces. We do this by evaporating a drop of concentrated latex particle suspension on a super-hydrophobic surface. The size of the obtained porous supra-particles after drying the suspension depends on the initial volume of the suspension drop.

We also discuss the potential implications of the different wettabilities of water-infused and oil-infused porous supra-particles on the type of Pickering emulsion stabilised by such particulates. The wettability results suggest that the pre-infusion of the same porous particles with oil or water may lead to different wettability and potentially different type of favoured emulsion.

Materials and methods

Materials

Surfactant-free polystyrene (PS) sulphate latex particles with diameter 2.5 ± 0.3 μm were obtained from Invitrogen as an 8.1 wt% aqueous suspension. Polystyrene has a density of 1.055 g cm^{-3} at 20 °C, a glass transition temperature (T_g) of 106 °C, and a refractive

index of 1.59 at 590 nm. These particles were soluble in benzene, chloroform, cyclohexane, toluene, acetone, and xylene but insoluble in ethanol, methanol, and water. The solubility data were used for choosing the best solvent with a negligible effect on the particle surface properties. Before use, the sulphate latex particles were washed two times with deionised water to remove any impurities. Activated aluminium oxide (STD grade, Merck) was used to remove any polar impurities from the oils. Potassium hydroxide (KOH, 99.6%) was supplied from Sigma. Dichlorodimethylsilane (DCDMS, 99.5%, GC) was obtained from Fluka. All aqueous solutions were prepared with de-ionised water obtained from a Millipore Milli-Q Plus water purification system through a 0.22 μm membrane. The water resistivity was around 18.2 MΩ cm^{-1}, the pH was 6.7, and the surface tension was 72.3 ± 0.6 mN m^{-1}, as measured by a drop shape analysis instrument (DSA MK10, Kruss).

Methods

Preparation of super-hydrophobic surfaces. Glassware was cleaned with a concentrated solution of KOH in ethanol for 1 hour, then washed with water and acetone in an ultrasonic bath for 10 min at room temperature and dried in an oven. Glassware surfaces were hydrophobized with DCDMS vapours by placing 1 mL of DCDMS and the glassware in a sealed box overnight, and then washing the glassware with hexane, which helped to remove any excess DCDMS from the glass surface. Hydrophobic fumed silica particles (AEROSIL® R202, Degussa) were dispersed in ethanol at 5 wt% using an ultrasonic probe (Model 450, Branson) operating at 50% amplitude with a 2 s pulse every 5 s for a total of 20 min. Then, approx. 0.5–1 mL of silica suspension was spread onto the glassware surfaces and dried for 20 min in an oven at 50 °C.

Preparation of composite porous supra-particles by manual rolling of latex suspensions on hot super-hydrophobic surfaces. Glass beakers with super-hydrophobic coating (see above) were used in these experiments. The composite porous particles were prepared using 2.5 ± 0.3 μm polystyrene sulphate latex particle suspensions with different concentrations in the range of 8.1–70 wt%. The concentrations above 8.1 wt% were prepared by settling the particles using a centrifuge at 4000 rpm for 3 min, removing a certain amount of the supernatant (water) and re-dispersing the particles. The concentrated suspension was degassed using a vacuum desiccator. Different volumes of latex particle suspensions (2.5–20 μL) were placed in a pre-heated beaker with a super-hydrophobic surface and rolled manually by moving the beaker on top of a hot plate set at 90 °C until the latex suspension droplet evaporated and dried (Fig. 1). The time needed to make one porous particle was between 1 and 10 min, depending on the initial concentration and volume of the particle suspension. Finally, the particles were fused together by heating in air at a temperature close to the glass transition temperature of polystyrene for a period of 30 min to 2 h as described below.

Annealing of the porous supra-particles. The following methods of temperature control for fusing the supra-particles in air at specific temperatures were investigated.
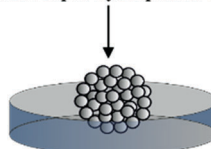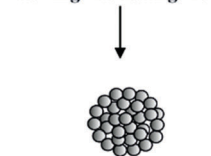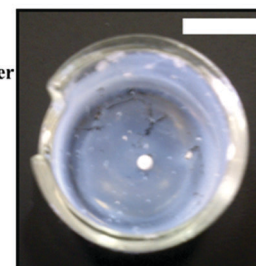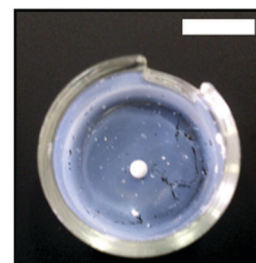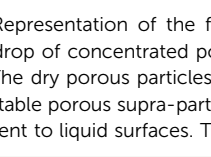

Fig. 1 Representation of the formation of a dry porous supra-particle from a drop of concentrated polystyrene latex suspension evaporated at 90 °C. The dry porous particles (2 mm) were partially fused at 106 °C to form a stable porous supra-particle used in our studies on porous particle attachment to liquid surfaces. The scale bars are 10 mm.

Fusing the particles using the hotplate method. The supra-particles are placed inside a dry sample tube immersed in an oil bath heated by a hot plate. The temperature of the bath was maintained at 107 °C by using a temperature probe immersed in the oil and connected to the hot plate control socket. The supra-particles obtained after 2 hours of heating by this method were stable in ethanol and water over a period of 24 hours.

Fusing the particles using a dry block heating system. In this method, the Grant (QBD1) dry block heating system was used to fuse the latex particles within the supra-particle. This system has interchangeable heating blocks, QB-E2, with a 35 mm-deep hole to fit a sample tube. Its temperature was first set at 103 °C and a dry sample tube containing the supra-particles was inserted in the heating block. After heating, the supra-particles were cooled to room temperature and placed in ethanol to test their stability. The supra-particles disassembled immediately, thus indicating that the latex particles were not fused together at this temperature. Increasing the temperature to 107 °C (which is just above the glass transition temperature of polystyrene, 106 °C) resulted in the formation of well-fused composite supra-particles, which were stable in both ethanol and water. Therefore, heating the supra-particles to 105–107 °C for 2 h was sufficient for fusing the building block particles. The produced supra-particles were stable after infusing with ethanol and water for 24 h.

Investigating the effect of temperature during evaporation of the latex suspension on the supra-particle structure. Droplets of sulphate latex particle suspension (15 μL of 50% w/w) were placed in pre-heated glass beakers and evaporated during manual rolling at temperatures of 60, 80 and 105 °C. The supra-particles obtained were put in a dry vessel inserted into an oil bath at 107 °C for 2 h to fuse the individual sulphate latex particles together. Images of the supra-particles formed were taken using a table top scanning electron microscope (SEM-TM1000, Hitachi) without coating the samples with carbon or gold.

Determining the packing density and porosity of supra-particles. To calculate the particle packing density and porosity of the supra-particles, their masses were measured twice, when dry and wet. The mass of the dry composite supra-particles was measured immediately after fusion, while their wet mass was measured after permeating the particles with ethanol in a desiccator followed by transfer into a beaker with water. The water-impregnated supra-particles were placed on a filter paper (Whatman) to remove the excess water on their surface. The wet mass of the particles was then measured by a precision balance (Sartorius). The supra-particle volume, V_p, was calculated from the dry mass, m_d, and the wet mass, m_w, using eqn (3) derived below.

The dry and wet masses of a supra-particle are given by eqn (1) and (2), respectively

$$m_d = V_p \phi \rho_{latex} \tag{1}$$

$$m_w = V_p \phi \rho_{latex} + V_p(1 - \phi)\rho_{water} \tag{2}$$

where ϕ is the latex volume fraction, ρ_{water} and ρ_{latex} are the densities of water and latex, respectively. From the above equations, the volume of the supra-particles can obtained:

$$V_p = \frac{m_w - m_d}{\rho_{water}} + \frac{m_d}{\rho_{latex}} \tag{3}$$

The supra-particle density, ρ_p, can be calculated by

$$\rho_p = \frac{m_d}{V_p} \tag{4}$$

The solid (latex) volume fraction of supra-particles was calculated as follows

$$\phi = \frac{m_d}{V_p \rho_{latex}}. \tag{5}$$

Impregnation of porous supra-particles with a fluid phase. The following method was used for impregnating the particles with water, hexadecane or air before attaching them to air–water and hexadecane–water interfaces. Impregnation with ethanol was the intermediate step in impregnating the particles with water. The porous supra-particles were impregnated with ethanol as air bubbles were found to move out from the pores. The particles were immersed in ethanol and the sample was placed in a vacuum desiccator for 10 min after which the particles were transferred to the bulk of deionised water (10–20 mL) and kept there overnight. The impregnation with oil was done by immersing the dry porous supra-particles into 10–20 mL of hexadecane, placed for 10 min in a vacuum

desiccator and then kept in the hexadecane overnight to ensure that the trapped air has been eliminated, and the pores were completely filled with the oil phase. Note that the hexadecane phase wets the dry porous particles as well as the ethanol phase and displaces the trapped air in their pores. Therefore, in the case of hexadecane-infusion there is no need for pre-wetting of the porous particle with ethanol as in the case of infusion with water.

Magnetic resonance imaging (MRI) method for determining the liquid front penetration in porous supra-particles attached to liquid interfaces. MRI is an imaging method[33] that uses a magnetic field and radio wave pulses to generate images of structures within the studied samples, which we utilise to probe the interior distribution of a liquid infused into the porous particles. The basis of the technique is a directional magnetic field associated with the atomic nuclei that possess an odd number of protons (*e.g.* hydrogen atoms) and have a precession. When the water-infused porous particle is exposed to a high magnetic field, a large fraction of the hydrogen nuclei align themselves with the field direction and precess around it with the Larmor frequency.[33] When a radio frequency pulse is applied perpendicular to the magnetic field with a frequency equal to that of the Larmor frequency, this causes the magnetic moment of the hydrogen nuclei to shift away from the direction of the applied magnetic field. Upon removal of the radio wave pulse the nuclei relax back to align themselves with the field direction and emit their own radio signal (free induction decay, FED) which is measured by a conductive field coil placed around the sample. The FED waves are then reconstructed to generate a 3D grey scale MR image. We used an MRI technique[33] to investigate the penetration of liquid into porous supra-particles with adequate resolution and satisfactory contrast. Porous supra-particles were used dry or initially infused with different fluids (hexadecane or water). We followed the impregnation procedure described in the previous section.

The studied porous supra-particle (~ 1 mm in diameter) was inserted into a capillary tube and then into a coil holder attached to the NMR probe. In a series of experiments, the porous supra-particle was first infused with water, and then placed in the middle of the capillary sample tube half-filled with deionised water. After that, the rest of the capillary tube was filled with hexadecane. In this setup, the supra-particle was in contact with the aqueous phase from one side and the oil-phase from the other side in a similar way as it would reside when attached to an oil–water interface. The purpose of this experiment was to evaluate the depth of penetration of the oil–water interface within the porous particle. This would give us important insight about how the pre-infused porous supra-particles attach at the liquid surface and if the liquid interface propagates inside during its attachment to this interface. The nuclear magnetic resonance (NMR) detects the presence of protons by applying a magnetic field to the samples. For that reason, the oil phase on the images has a brighter colour than water, due to variation in proton density, thereby decreasing the contrast inside the particle. A composite supra-particle was placed in this setup and imaged using a Bruker AVANCE 2 wide
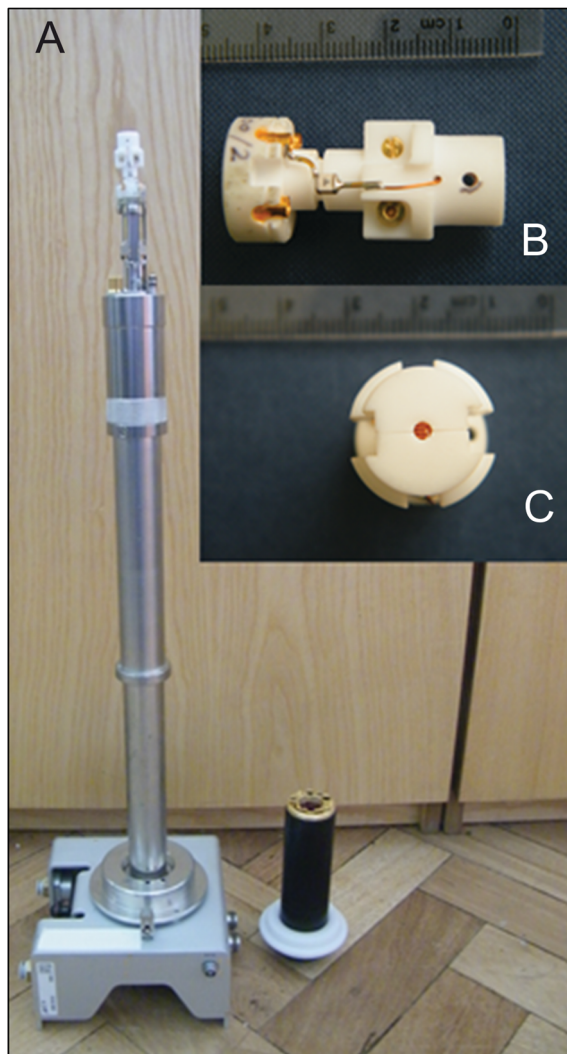
Fig. 2 (A) Photograph of the probe used for the MRI experiment to visualise the penetration of liquid into the porous particles. Insets show side (B) and top (C) photographs of the solenoid coil which is attached to the top of the Bruker microimaging probe shown in (A).

Fig. 3 Optical images of supra-particles formed by evaporation of sulphate latex suspension of various particle concentrations (8–70 wt%, shown) on a super-hydrophobic surface at 90 °C. The latex suspension drop was rolled over the hot super-hydrophobic surface until complete evaporation occurred. All scale bars are 0.50 mm.

bore 11.74 T magnet fitted with a Bruker microimaging probe with a 2 mm solenoid coil (Fig. 2). Standard pulse sequences from the Bruker Paravision library were used. Multi Spin Multi Echo (MSME) sequences were acquired using the solenoid coil and Bruker's MSME_Bas sequence. The image slice thickness was 0.17 mm, and the resolution was about 20 μm (per pixel). The readings were taken under constant temperature of 20 °C. It took approximately 1 hour to capture each image.

Results and discussion

Model supra-particles made by rolling particle suspension on the super-hydrophobic surface

Porous supra-particles with different shapes were successfully produced by using a hot super-hydrophobic glass surface and different initial latex particle concentrations. The initial particle concentration in the latex suspension turned out to be an
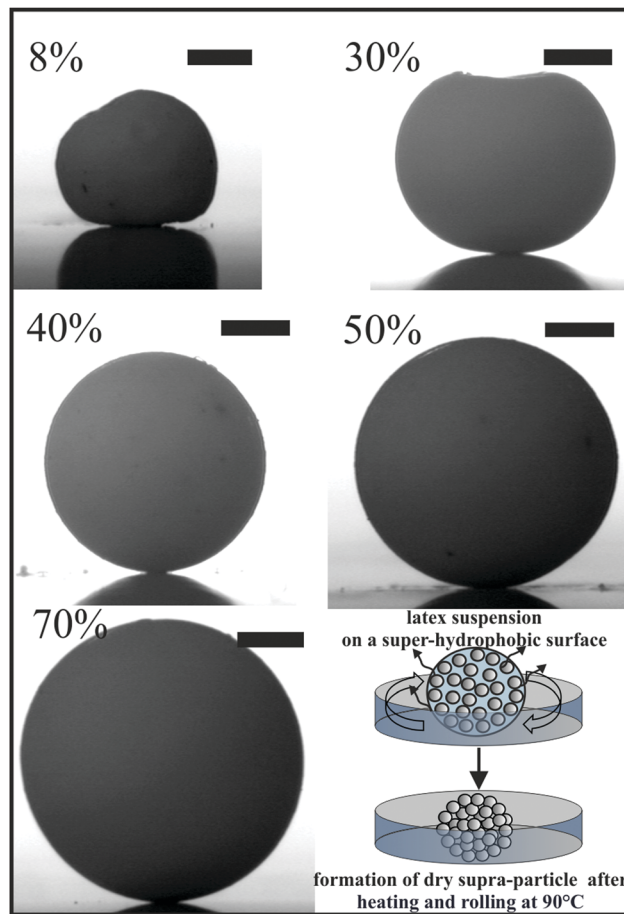
important factor in determining the final shape of the porous particles. The particles formed from evaporating 20 μl drops of a latex suspension at concentrations 8.1% and 30% produced shape-anisotropic particles, while the same amount of latex suspension of higher concentrations (40%, 50% and 70 wt%) produced spherical particles, with diameters 2.1 mm, 2.2 mm and 2.4 mm, respectively (see Fig. 3).

Characterisation of the supra-particle morphology

The surface structure and the porosity of the porous supra-particles are affected by the initial concentration of the sulphate latex particle suspension. Fig. 4(A and B) reveals that the supra-particles produced from 8.1 wt% latex particle suspension have a randomly packed porous structure. As expected, upon increasing the particle concentration, the latex particles started forming a close-packing structure. At 40 wt% latex particles, as shown in Fig. 4C and D, a much smoother supra-particle surface was formed with some large pores. Fig. 5 shows that at latex particle concentrations ≥ 50 wt%, close-packed structures with much lower porosity were produced on the supra-particle surface. Also, the number of defects (large pores) in the produced supra-particles
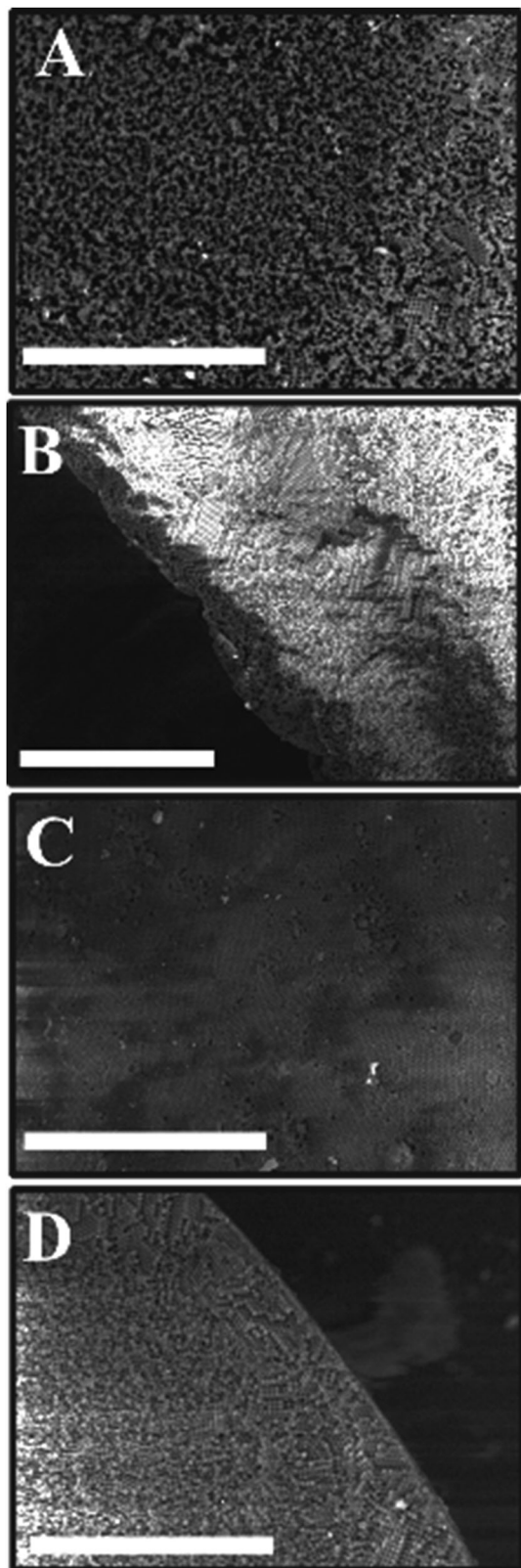
Fig. 4 SEM images of supra-particles made from much smaller sulphate latex particles (2.5 μm in diameter) by evaporation of latex suspensions with concentrations (A and B) 8.1 wt%, and (C and D) 40 wt%. (A) and (C) show the outer surface morphology of supra-particles; (B) and (D) show the inner structure near the edge of sectioned supra-particles. All scale bars are 100 μm.
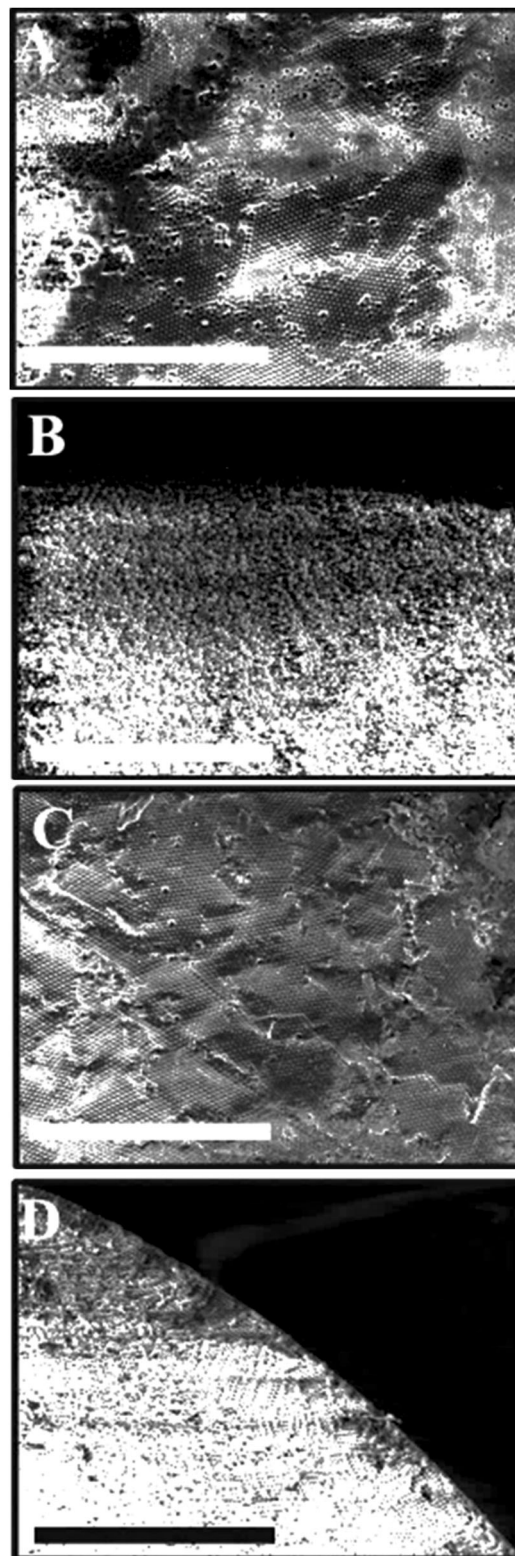
Fig. 5 SEM images of the surface of supra-particles made from 2.5 μm sulphate latex particles. The SEM images in (A) and (C) show the outer surface morphology of the supra-particles prepared from (A) 50 wt%, and (C) 70 wt% latex suspension. The supra-particles in (B) and (D) were sectioned to reveal the internal structure of the latex particle assembly near the supra-particle surface. The scale bar is 100 μm in all images.

is much smaller than those at lower particle concentrations. Such results, to the best of our knowledge, have not been reported by other authors before and the dependence of the supra-particle surface morphology on the small particle concentration has not been discussed in the existing literature.[17,28]

The surface morphology of supra-particles produced from 70 wt% latex particle suspension shows much more compact structures, resulting in a rough but less porous surface (Fig. 5C and D). Supra-particles made from 40–70 wt% latex suspensions showed colloidal crystalline domains on their surface. The inner structure of the packed latex particles was investigated using a SEM, as seen in (Fig. 4 and 5B, D) at the edge of the porous supra-particles. The supra-particles were fractured with a scalpel blade to focus on latex particle assemblies at the edge of the section. Supra-particles obtained from 8.1 wt% latex particle suspension show significantly less ordered layers of composite sulphate latex as a result of the increased volume fraction of water in the process of supra-particle formation (Fig. 4B). However, when the initial latex particle concentration increases, the edge structure of the formed supra-particle starts to show more densely packed structures (Fig. 4D).

The temperature of the hot super-hydrophobic surface during the evaporation of the latex suspension is also expected to control the surface morphology of the produced model supra-particles. We tested this effect at several temperatures up to the polymer glass transition temperature. The SEM images in Fig. 6 show that the latex particles start to be packed and organised with increasing temperatures from 60 to 105 °C.

However, the inner structure of the assembled latex particles shows that they are still randomly packed as the suspension gets jammed on the surface of the evaporating drop before the same phenomenon occurs in the core. Hence, the latex particles in the core can rearrange in a larger volume than those in the surface layer, which results in random packing in the core of the produced supra-particles (see Fig. 6A and B).

Thermal annealing of the porous supra-particles

Latex particle fusion in the assembled supra-particles is affected by temperature. If the particles are held at temperatures above the glass transition temperature for polystyrene latex $T_g = 106$ °C, i.e. $T > T_g$, the polystyrene particles started to partially melt, the polymer turned soft and they fused together in an aggregate (Fig. 7). When the latex particles were partially fused, they showed a glassy appearance and changed their composite colour to yellowish. Note that extensive fusion and melting of the latex particles would block all the pores and would not allow us to characterise the effect of the particle porosity on its three-phase contact angle at liquid surfaces. We found that this was the case with particles annealed at 120 °C where the supra-particles melted and formed glassy supra-particles (e.g. compare Fig. 7B and D). However, supra-particles annealed below 103 °C were found to have poor stability and disintegrated when infused by a solvent (both water and oil).

Characterisation of the supra-particles' density and porosity

We studied how the supra-particles mass density and the corresponding porosity depend on the initial particle concentration of the latex suspension. We found that the supra-particle packing density increased steeply with increasing of the initial
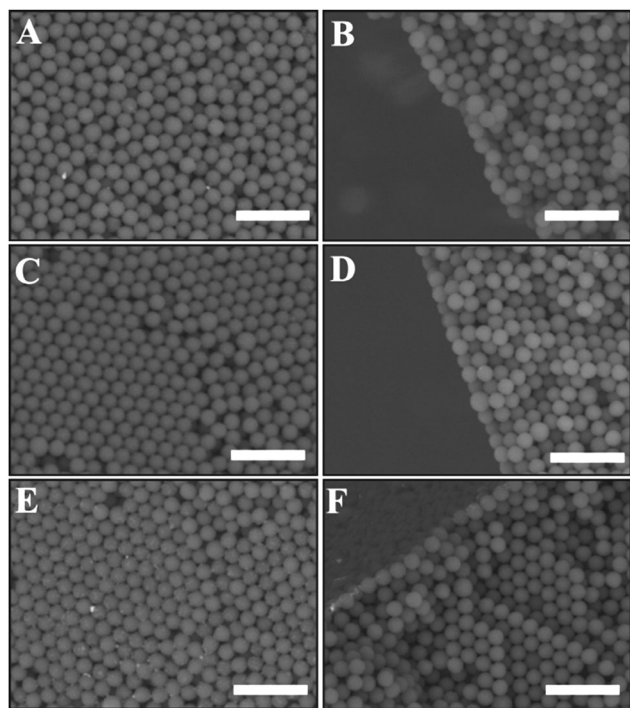

Fig. 6 SEM images of porous supra-particles made by evaporating drops of 50 wt% latex suspension on a hot super-hydrophobic surface, heated at 60 °C (A and B), 80 °C (C and D) and 105 °C (E and F). Surface morphology (A, C and E), and the inner structure at the edge of fragmented supra-particles (B, D, and F) can be seen. The scale bar in all images is 10 μm.
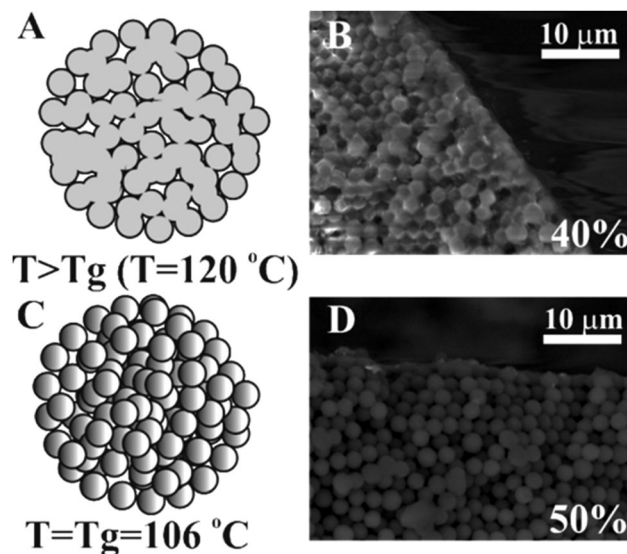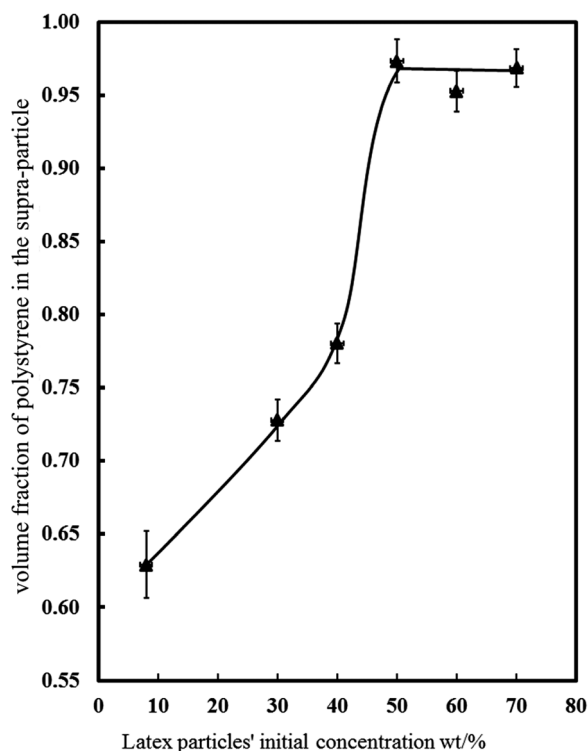

Fig. 7 Illustration of the effect of temperature on the fusion of individual polystyrene latex particles inside a composite supra-particle: (A) a diagram of the fusion of latex particles annealed at $T > T_g$; (B) a SEM image of a supra-particle made from a 40 wt% latex particle suspension annealed at 120 °C; (C) a diagram of a supra-particle annealed at the glass transition temperature (T_g) of polystyrene (106 °C); (D) a SEM image of a fractured porous supra-particle made from 50 wt% particle suspension after annealing at T_g.

Table 1 Mass density and solid volume fraction of porous supra-particles obtained by drying and annealing of latex particle suspension at various concentrations. The annealing temperature was 106 °C for all particles. The mass-density and porosity of the supra-particles were determined as described above. Here, ϕ is the latex particle volume fraction in the supra-particle calculated from the mass measurements by eqn (5) and ρ_p is the supra-particle mass density calculated by eqn (4)

Latex particle initial concentration/wt%	ρ_p/g cm^{-3}	ϕ
8.1	0.793 ± 0.020	0.629
30	0.853 ± 0.008	0.728
40	0.883 ± 0.010	0.780
50	0.987 ± 0.001	0.973
60	0.976 ± 0.002	0.953
70	0.984 ± 0.010	0.968

latex particle concentration. The highest packing density was obtained from 50 wt% latex suspension and remained unchanged for further increases in the particle concentration (60 wt% and 70 wt%). The values of the particle density and porosity were calculated by using eqn (4) and (5), respectively. Table 1 summarises the mass densities and the volume fraction of latex particles in the obtained supra-particles as a function of the initial concentration of the latex suspension used to build these supra-particles. As expected, supra-particle porosity $(1 - \phi)$ decreases when the concentration of the latex particles in the initial suspension is increased. Fig. 8 presents the same data

for the volume fraction of the latex particles *versus* the initial latex concentration.

As demonstrated in Fig. 3, we need a minimum of 40 wt% latex particles in the suspension in order to make spherical porous particles. Lower latex particle concentration in the suspension led to the formation of non-spherical supra-particles, which were not desirable for our purposes. On the other hand, since we also want to partially fuse the latex particles and form a stable supra-particle while still maintaining the particle porosity, there is a trade-off between the initial latex particle concentration and the final supra-particle porosity. As Fig. 8 shows, the supra-particle porosity sharply decreases above 50 wt% due to the colloid crystalline nature of the packed latex particles at higher concentrations which after partial fusion leave very small voids in between them. This is also undesirable for our purpose to produce model porous particles and shows that we have limited control over the supra-particle porosity while still maintaining their spherical shape and stability. Therefore, we chose to study only model supra-particles obtained by evaporation of the optimal concentration of 40 wt% latex particle suspension on a super-hydrophobic surface followed by thermal annealing at the polystyrene glass transition temperature. These supra-particles were spherical and showed very good stability when infused with ethanol, water and hexadecane, while having at least $1 - \phi = 0.22$ volume fraction of pores (voids) in between their partially fused latex particle building blocks (see Fig. 8).

Observation of impregnation of the supra-particles with liquids

In order to find the best method to impregnate the pores of the supra-particles with liquids, two different experiments were carried out. The particles were pre-wetted in ethanol for 5 min and then immersed in 10^{-5} M aqueous solution of Rhodamine 6G for 30 min or overnight. Optical and confocal fluorescence microscopy was used to observe the liquid phase penetration in the pores of the supra-particles. The results with optical fluorescence microscopy are presented in Fig. 9 which shows incomplete infusion after 1 hour but complete infusion after overnight incubation in the aqueous Rhodamine 6G solution. This delayed infusion can be explained by the slow dissolution of the dye inside of the supra-particle as it is inserted in the liquid phase. We also used an infusion with silver nitrate solution as a tracer
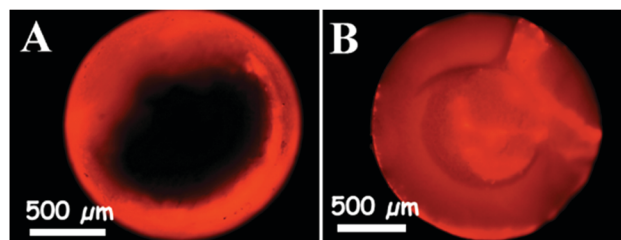

Fig. 8 Relation between the latex particles' initial concentration in w/w% (*x*-axis) and the volume fraction of sulphate latex particles in the supra-particles (*y*-axis). The volume fraction of these particles increased with the increase in the particles' initial concentration and reduced the pore fraction of the total particles. Above 50 wt%, the latex particle volume fraction levelled off.

Fig. 9 Fluorescence microscopy images of a porous supra-particle impregnated with 10^{-5} M Rhodamine 6G solution after (A) 1 hour and (B) overnight. The particles were fragmented after infusion with the liquid before being observed and imaged on a fluorescence microscope using a TRITC filter set. Particles were obtained from a 40 wt% latex suspension (see Table 1 for more details).
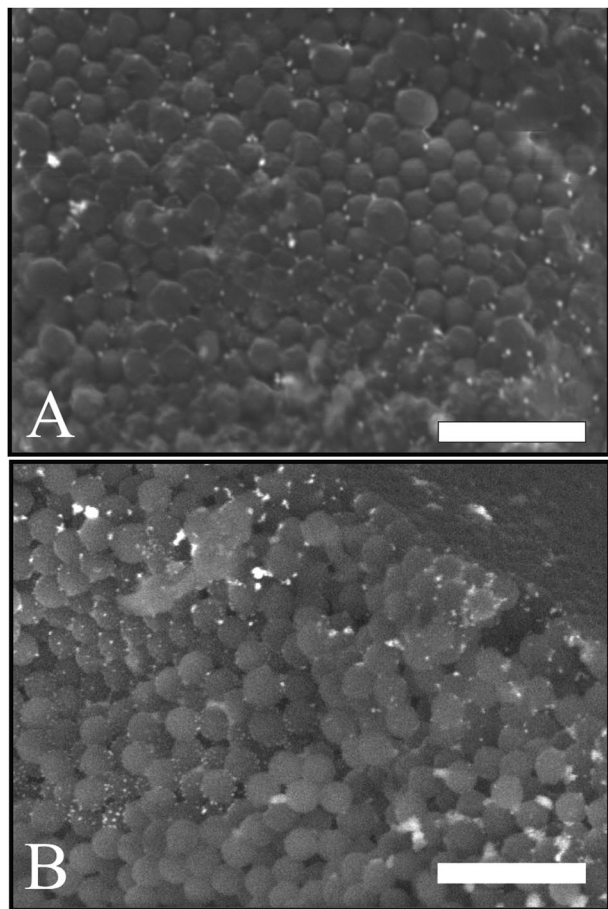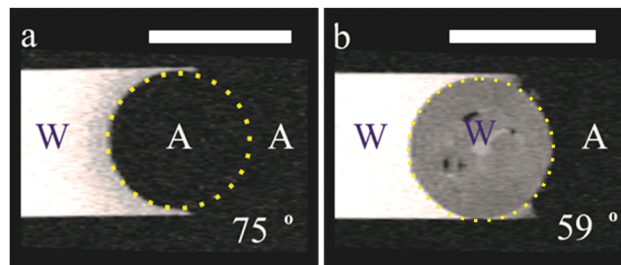
Fig. 10 SEM images represent the infusion of an aqueous solution of silver nitrate inside the pores of a supra-particle; (A) is a SEM image of the supra-particle's outer surface, while (B) is a SEM image of the inner structure at the edge of a fractured supra-particle. The particles were removed from the solution and dried up before imaging. Silver nitrate nanocrystals appear as bright spots on the images. The scale bars are 10 μm.

Fig. 11 MRI images of composite porous supra-particles made from 40% 2.5 μm sulphate latex particle suspension by the evaporation and thermal annealing method (see Table 1 for particle parameters). The image shows the position of the air–water (A–W) surface on the porous particle surface. (a) A dry supra-particle attached at the A–W interface; pores are filled with air, as the air shows a dark region; (b) a water infused supra-particle attached to the A–W interface; water inside the porous particle is seen in grey colour. The particles show different resolutions when infused with water, as the interior of the particle becomes grey, the liquid water corresponds to white and the air has been represented by a black colour. The approximate values of the apparent supra-particle contact angle shown have been estimated from the images (for details see the text). The scale bars are 1 mm.

to investigate whether the water phase penetrated completely throughout the supra-particles. Fig. 10 shows SEM images for supra-particles incubated with 0.1 M silver nitrate aqueous solution which, after drying, show the silver salt crystals as white dots on the outer surface of the latex particles and inside the porous supra-particle. These experiments show that it is very difficult to displace the air from a dry porous supra-particle with water and the only effective way is to use an intermediate solvent (ethanol) and dissolve the air into the liquid as an alternative to evacuating the trapped air by vacuum desiccation.

Magnetic resonance imaging for porous supra-particles at fluid–liquid interfaces

Dry and water-wet composite porous supra-particle attachment at the air–water interface. The aim of these experiments was to visualise the position of the air–water front penetration inside the porous supra-particles when a dry or a wet supra-particle was attached to the air–water interface. The black region inside the supra-particle imaged by MRI (Fig. 11a) shows that there is no water present inside the pores of the particle.

The liquid water phase appears on the MRI images (Fig. 11a and b) as a brighter colour than the water trapped inside the particle pores (Fig. 11b), as the shade of grey on the image is affected by the relaxation time of the hydrogen atoms in the magnetic field. In this setup the hydrogen atoms of free water molecules have different relaxation times than the hydrogen atoms in the polystyrene particles which are fixed in the porous supra-particle. The air phase appears in black colour on these images. The particle three-phase contact line diameter was difficult to determine with high enough precision and to observe directly due to the curvature of the liquid meniscus in the capillary tube. Approximate values of the particle contact angle were obtained from the image by drawing a circle around the particles and presuming that the grey colour near the air–water interface is the contact line diameter. The images in Fig. 11 do not indicate that there is penetration of water in the dry porous particles (Fig. 11a) as well as no penetration of air in the water-wet porous particles (Fig. 11b) upon their attachment at the air–water interface.

To get more information about the attachment of supra-particles to macroscopic air–water interfaces, we performed optical observations in addition to the MRI study. The air–water interface was formed at the tip of a glass tube connected to a syringe. In the experiments with dry supra-particles, the tube was filled with water and the air–water interface was adjusted to be almost flat by using the syringe. The dry supra-particle was placed in air at the bottom of a glass cuvette. It was attached to the air–water surface by lowering the tube until the particle became partially immersed in the water. Similarly, in the experiments with wet supra-particles, a supra-particle impregnated with water was placed in a cuvette filled with water. The tube was filled with air and the air–water interface was adjusted to be almost flat by using the syringe. Then the tube was lowered until the particle became partially immersed in the air inside the tube. Side images of supra-particles attached to the air–water interface taken using
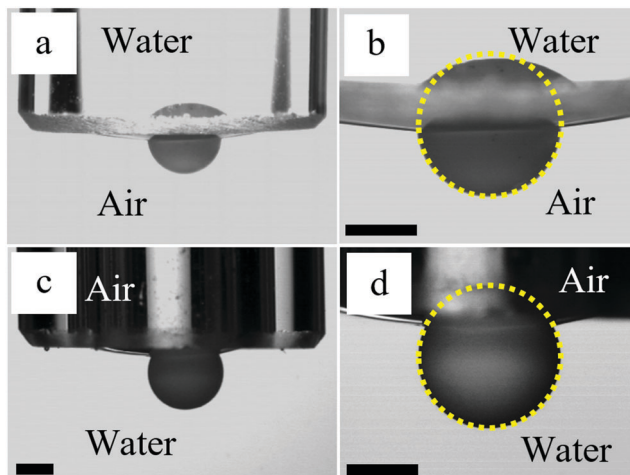
Fig. 12 Optical side images of supra-particles attached to the air–water interface at the tip of a glass tube with inner diameter 5 mm connected to a syringe (not shown). (a and b) The dry supra-particle in air is attached to the air–water surface by lowering the glass tube filled with water. (c and d) The wet supra-particle in water is attached to the air–water surface by lowering the glass tube filled with air. (b and d) Enlarged images of the supra-particles shown in (a and c), respectively. Contact angles through water estimated from the images are $77 \pm 3°$ (a and b) and $60 \pm 4°$ (c and d). The composite porous supra-particles shown have been made from a 40 vol% 2.5 μm sulphate latex particle suspension by the evaporation and thermal annealing method (see Table 1 for particle parameters). The scale bars are 1 mm.

a CCD camera are shown in Fig. 12. We could not assess the penetration of the outer fluid inside the porous supra-particles in these experiments, but the contact angles estimated from the images are in good agreement with those observed in the MRI experiments (see Fig. 11).

Water-wet and oil-wet porous supra-particles attached at the oil–water interface. The brightness of the produced MRI images is higher at places with protons with shorter relaxation time.[33] When adding oil (*i.e.* hexadecane), the contrast and resolution change because of the amount of hydrogen in the oil. In the MRI images of a supra-particle infused by oil (hexadecane) attached to the oil–water interface (Fig. 13), the colour of the bulk water phase is bright white; the water inside the particle pores appears grey and the air region as a black colour. When adding oil to the
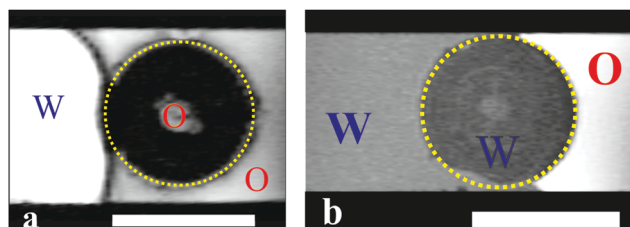
particle–water interface, the whole particle in the MRI image turns into a dark grey colour because of the higher contrast in the oil, which decreases the contrast of water outside and inside the porous particle. The images in Fig. 13 do not indicate that there is penetration of water in the oil-infused porous particles (Fig. 13a) as well as no penetration of oil in the water-infused porous particles (Fig. 13b) upon their attachment at the oil–water interface.

Oil-wet porous supra-particles at the air–oil interface. Here, the porous supra-particle was initially impregnated with oil, then inserted into the capillary tube and suspended at the oil–air interface (Fig. 14). When the particle was inside the glass capillary, a microsyringe needle was used to gently push the particle towards the oil–air interface. Note that in the image the oil-infused particle is barely touching the oil–air surface, which indicates a very low value of particle contact angle at this (A/O) liquid interface. We were not successful to attach a dry porous supra-particle at the oil–water interface as the particles were completely transferred to the oil phase.

These experiments illustrated in Fig. 11 and 13 suggest that the supra-particle attachment at the air–water or the oil–water interface occurs only on the supra-particle surface layer of latex particles without a deep penetration of the liquid–fluid interface front into the porous particle interior. If the porous supra-particle is initially dry, it remains dry upon attachment at the air–water interface. If the porous particle is pre-wet, its interior remains water-wet after attachment at both the air–water and oil–water interfaces. These findings conform to Scheme 1 that illustrates the perceived mechanism of the attachment of porous particles pre-infused with different fluid phases (oil or water for the oil–water interface as well as air or water for the air–water interface). In the MRI images, we do not see a penetration of the adjacent liquid phase inside the porous supra-particle and a displacement of the infusing liquid (oil or water) upon its attachment to the liquid–fluid interface. The consequences of this is that porous particles would attach only on the outer layer of small particles (building blocks) and would exhibit a different effective contact angle depending from which fluid phase they approach the liquid–fluid interface (see Scheme 1).

This attachment mechanism may not be different for particles of varying porosities. The reason is that after the initial attachment, which is equivalent to the adsorption of a fraction of the outer layer of building block particles on the surface of the supra-particle,
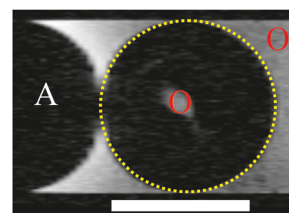

Fig. 13 MRI images for porous supra-particles pre-infused with: (a) oil (hexadecane) and (b) water, followed by the particle attachment to the oil–water interface from the original liquid phase. The scale bars are 1 mm. The composite porous supra-particles made from a 40 vol% 2.5 μm sulphate latex particle suspension by the evaporation and thermal annealing method (see Table 1 for particle parameters).

Fig. 14 A MRI image of a supra-particle filled with oil (hexadecane) at the oil–air interface. We cannot identify an imbibition of air in this image, as the interior of the particle does not change upon attachment to the air phase. The composite porous supra-particle shown here was made from 40 vol% 2.5 μm sulphate latex particle suspension by the evaporation and thermal annealing method (see Table 1 for particle parameters). The scale bar is 1 mm.
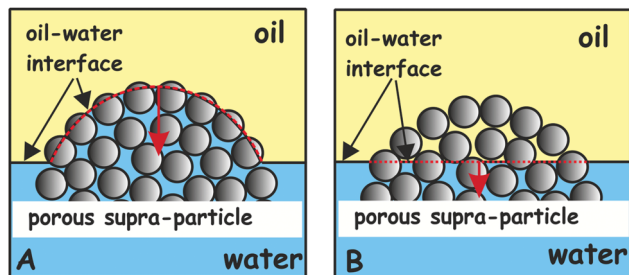
Scheme 2 Effect of the pinning of the oil–water interface on the first-layer of building block-particles on the surface of the porous supra-particle. (A) The porous supra-particle has been pre-infused with water before its attachment to the oil–water interface. The position of the layer is shown schematically with a red-dashed line. (B) The potential penetration of the oil–water interface further into the porous particle core requires detachment of the outer layer of small particles which needs energy much higher than the thermal energy, kT. This is why (A) is the preferred mechanism of attachment.

the further movement of the fluid–liquid front within the porous particle core would require the desorption of the first layer of adsorbed small particles from the liquid interface. This process, however, is thermodynamically disfavoured, as it requires energy much higher than the thermal energy, kT, per latex particle to detach. This leads to an effective pinning of the liquid–fluid interface on the outer layer of small particles at the surface of the supra-particle pre-infused with the surrounding fluids.[34] Scheme 2 illustrates the pinning effect of the first layer of particles of the surface of the porous supraparticle. Our results are consistent with the similar findings from the GTT for aggregates of hydrophobised silica particles.[23] Recently, Paunov et al.[35] developed a theoretical model for the attachment of a porous composite particle aggregate which predicts a different contact angle of the particle depending on which liquid (oil or water) it is initially pre-infused with. Their theory allowed to link the contact angle of the aggregate building block particles with the contact angle of the liquid-preinfused aggregate at the oil–water interface. That theory was experimentally tested and the measured contact angles of the porous composite particles were in good agreement with prediction of the theory based on the value of the contact angle of the small particle building blocks. MRI images from our experiments also suggest that if the supra-particle was oil-infused, it remained oil-wet after attachment to the oil–water interface, while the oil–water interface was attached on the outer layer of the latex particle.

These results call for some discussion about the potential implication of the pre-infusion of the porous particles (or particle aggregates) with oil or water on their behaviour as stabilisers of Pickering emulsions. Scheme 3 shows the potential effect of infusion of porous particles with water (Scheme 3A) and oil (Scheme 3B) on the type of emulsion. Since the use of hydrophilic particles generally favours oil-in-water emulsion, the pre-infusion of the porous particles with the aqueous phase can make the original particles more hydrophilic. In contrast, since hydrophobic particles usually favour the formation of water-in-oil emulsions, the pre-infusion of the porous particles with the oil phase can make them more hydrophobic. Experimental results with using
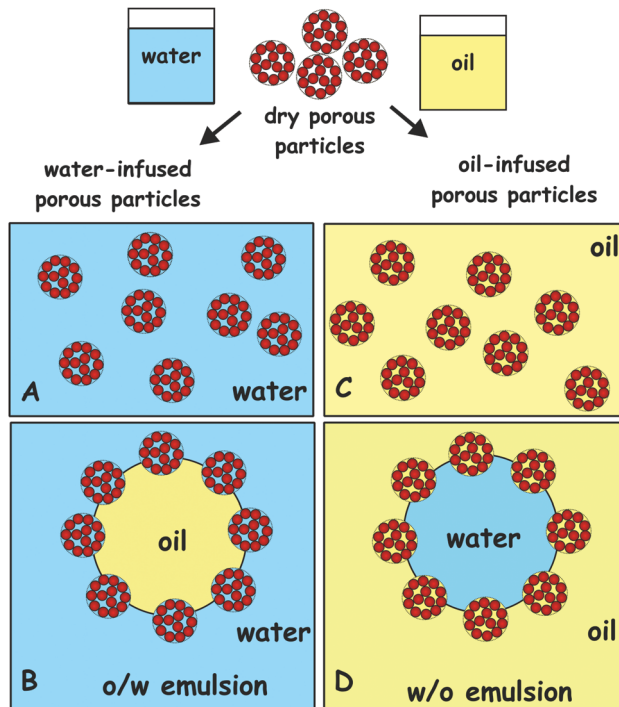
Scheme 3 Effect of the pre-infusion of the porous particles with water (A) and oil (C) on the favoured type of Pickering emulsion obtained upon using the pre-infused porous particles as emulsifiers: (B) oil-in-water emulsion and (D) water-in-oil emulsion.

aggregated particles as emulsifiers have been reported in the literature and give different results depending on the initial liquid phase with which the particles are mixed and introduced in the system.[36–38] Therefore, oil-in-water Pickering emulsion could potentially be obtained with the water-infused porous particles as stabilisers while the used of oil-infused particles could yield water-in-oil Pickering emulsion at the same conditions (see Scheme 3).

Binks et al. demonstrated a phase inversion of a Pickering emulsion using the powdered fumed silica particles around 90° contact angle of the powdered particles.[39] Nonomura et al. showed that multiple Pickering emulsions can be produced using hollow particles as stabilisers depending on what liquid they are first introduced with.[40] Clegg et al. showed recently that multiple Pickering emulsions can be obtained in one step by a microfluidic method where fluid is trapped together with the particles.[41] All these authors indicate that aggregates of particles appear to be important for the formation of Pickering multiple emulsions in a single step. Trapped liquid within particle aggregates or porous particles could be a viable explanation. The experimental results in the present paper might provide strong support for this explanation.

Conclusions

Porous composite supra-particles were prepared by evaporation of a sulphate latex suspension on a hot super-hydrophobic surface. Non-spherical or near spherical supra-particle shapes were obtained, depending on the suspension drop evaporation technique used.

The supra-particles were thermally annealed close to the polymer glass transition temperature in order to partially fuse the latex particle building blocks. This technique allows control over the supra-particle size by changing the drop evaporation temperature and droplet concentration and volume. Using a latex suspension of particle concentration below 40 wt% produced supra-particles with non-spherical shape. However, using a suspension of higher concentration, 40–70 wt%, near spherical porous supra-particles were successfully produced. The supra-particles obtained had a rough surface, with a porous and amorphous structure. The supra-particle surface morphology and the inner structure were characterised by SEM imaging. The porosity of the porous supra-particles was controlled by the volume and the initial concentration of the latex particles' suspension and the rate of evaporation. Annealing of the supra-particles at the glass transition temperature of polystyrene did not cause significant changes in their appearance but fused the latex particles together to form a stable rigid porous supra-particle. Annealing at higher temperatures formed hard, completely fused supra-particles of glassy appearance. The effect of the suspension concentration on the supra-particle mass density and porosity was investigated. It was found that when the initial latex particle concentration was above 40 wt%, the obtained supra-particles became much denser and less porous than those obtained from more diluted latex suspensions. The penetration of water inside the porous spherical supra-particles upon incubation in aqueous solutions was studied by using aqueous fluorescent tracers and solutions of heavy metal salts. The timescale of complete infusion with water due to the existence of trapped air in the supra-particle upon incubation was demonstrated. MRI was used as a method for localising the air–water and oil–water interfaces in the pores of dry and pre-wet supra-particles. The MRI results indicate that the liquid–fluid interface does not penetrate through the supra-particle interior pores. The particle attachment at the air–water and oil–water interfaces occurs through the adsorption of the surface layer of colloid particles constituting the composite porous supra-particle surface. These results demonstrate the mechanism of attachment of densely packed particle aggregates at liquid surfaces and could be helpful for better understanding of the attachment of aggregated particles on the surface of emulsion droplets and particle-stabilised foams.

Acknowledgements

References

1 P. Klobes, K. Meyer and R. G. Munro, *NIST recommended practice guide: porosity and specific surface area measurements for solid materials*, NBS Special Publication 960-17, National Institute of Standards and Technology, 2006.

2 K. S. W. Sing, D. H. Everett, R. A. W. Haul, L. Moscou, R. A. Pierotti, J. Rouquerol and T. Siemieniewska, *Pure Appl. Chem.*, 1985, **57**, 603–619.

3 J. Haber, Manual on Catalyst Characterization, *Pure Appl. Chem.*, 1991, **63**, 1227–1246.

4 D. Everett, *Pure Appl. Chem.*, 1972, **31**, 577–638.

5 G. Nichols, S. Byard, M. J. Bloxham, J. Botterill, N. J. Dawson, A. Dennis, V. Diart, N. C. North and J. D. Sherwood, *J. Pharm. Sci.*, 2002, **91**, 2103–2109.

6 J. J. Cong, Y. Z. Chen, J. Luo and X. Y. Liu, *J. Solid State Chem.*, 2014, **218**, 171–177.

7 O. D. Velev, A. M. Lenhoff and E. W. Kaler, *Science*, 2000, **287**, 2240–2243.

8 V. N. Paunov and O. J. Cayre, *Adv. Mater.*, 2004, **16**, 788–791.

9 A. D. Dinsmore, M. F. Hsu, M. G. Nikolaides, M. Marquez, A. R. Bausch and D. A. Weitz, *Science*, 2002, **298**, 1006–1009.

10 N. P. Ashby, B. P. Binks and V. N. Paunov, *Phys. Chem. Chem. Phys.*, 2004, **6**, 4223–4225; K. L. Thompson and S. P. Armes, *Chem. Commun.*, 2010, **46**, 5274–5276.

11 O. J. Cayre, P. F. Noble and V. N. Paunov, *J. Mater. Chem.*, 2004, **14**, 3351–3355.

12 V. N. Paunov, P. F. Noble, O. J. Cayre, R. G. Alargova and O. D. Velev, *MRS Proceedings*, 2004, **845**, AA5.18.1-5.

13 P. F. Noble, O. J. Cayre, R. G. Alargova, O. D. Velev and V. N. Paunov, *J. Am. Chem. Soc.*, 2004, **126**, 8092–8093.

14 K. L. Thompson, S. P. Armes, J. R. Howse, S. Ebbens, I. Ahmad, J. H. Zaidi, D. W. York and J. A. Burdis, *Macromolecules*, 2010, **43**, 10466–10474.

15 K. L. Thompson, E. C. Giakoumatos, S. Ata, G. B. Webber, S. P. Armes and E. J. Wanless, *Langmuir*, 2012, **28**, 16501–16511.

16 K. L. Thompson, E. C. Giakoumatos, S. Ata, G. B. Webber, S. P. Armes and E. J. Wanless, *Langmuir*, 2012, **28**, 16501–16511.

17 V. Rastogi, S. Melle, O. G. Calderon, A. A. Garcia, M. Marquez and O. D. Velev, *Adv. Mater.*, 2008, **20**, 4263–4268.

18 Y. S. Cho, S. H. Kim, G. R. Yi and S. M. Yang, *Colloids Surf., A*, 2009, **345**, 237–245.

19 S. M. Klein, V. N. Manoharan, D. J. Pine and F. F. Lange, *Langmuir*, 2005, **21**, 6669–6674.

20 O. D. Velev, K. Furusawa and K. Nagayama, *Langmuir*, 1996, **12**, 2374–2384.

21 O. D. Velev, K. Furusawa and K. Nagayama, *Langmuir*, 1996, **12**, 2385–2391.

22 Y. Xia, T. D. Nguyen, M. Yang, B. Lee, A. Santos, P. Podsiadlo, Z. Tang, S. C. Glotzer and N. A. Kotov, *Nat. Nanotechnol.*, 2011, **6**, 580–587.

23 D. M. Kuncicky, K. Bose, K. D. Costa and O. D. Velev, *Chem. Mater.*, 2007, **19**, 141–143.

24 J. Park, J. Moon, H. Shin, D. Wang and M. Park, *J. Colloid Interface Sci.*, 2006, **298**, 713–719.

25 Y. Zhao, X. Zhao, C. Sun, J. Li, R. Zhu and Z. Gu, *Anal. Chem.*, 2008, **80**, 1598–1605.

26 G. R. Yi, S. J. Jeon, T. Thorsen, V. N. Manoharan, S. R. Quake, D. J. Pine and S. M. Yang, *Synth. Met.*, 2003, **139**, 803–806.

27 V. Rastogi, A. A. Garcia, M. Marquez and O. D. Velev, *Macromol. Rapid Commun.*, 2010, **31**, 190–195.

28 S. H. Kim, J. M. Lim, S. K. Lee, C. J. Heo and S. M. Yang, *Soft Matter*, 2010, **6**, 1092–1110.

29 O. J. Cayre and V. N. Paunov, *Langmuir*, 2004, **20**, 9594–9599.

30 V. N. Paunov, *Langmuir*, 2003, **19**, 7970–7976.

31 V. N. Paunov and O. J. Cayre, *MRS Proceedings*, 2003, M8.25.1-3.

32 L. A. Arnaudov, O. J. Cayre, S. D. Stoyanov, M. Cohen-Stuart and V. N. Paunov, *Phys. Chem. Chem. Phys.*, 2010, **12**, 328–331.

33 T. Neuberger and A. Webb, *NMP Biomed.*, 2009, **22**, 975–981.

34 N. P. Ashby, B. P. Binks and V. N. Paunov, *Chem. Commun.*, 2004, 436–437.

35 V. N. Paunov, H. Al-Shehri and T. S. Horozov, *Phys. Chem. Chem. Phys.*, 2016, DOI: 10.1039/c6cp05453f.

36 B. B. Binks and S. O. Lumsdon, *Phys. Chem. Chem. Phys.*, 2000, **2**, 2959–2967.

37 B. P. Binks and J. A. Rodrigues, *Langmuir*, 2003, **19**, 4905–4912.

38 B. P. Binks, J. Philip and J. A. Rodrigues, *Langmuir*, 2005, **21**, 3296–3302.

39 B. P. Binks, P. D. I. Fletcher, B. L. Holt, P. Beaussoubre and K. Wong, *Phys. Chem. Chem. Phys.*, 2010, **12**, 11954–11966.

40 Y. Nonomura, N. Kobayashi and N. Nakagawa, *Langmuir*, 2011, **27**, 4557–4562.

41 P. S. Clegg, J. W. Tavacoli and P. J. Wilde, *Soft Matter*, 2016, **12**, 998–1008.